Inorg. Chem. **2005**, *44*, 9542–9546

First Structural Characterization of a Protactinium(V) Single Oxo Bond in Aqueous Media

Claire Le Naour,[†] Didier Trubert,[†] Maria V. Di Giandomenico,[†] Clara Fillaux,[‡] Christophe Den Auwer,*[,‡] Philippe Moisy,[‡] and Christoph Hennig[§]

Centre National de la Recherche Scientifique/IN2P3/Paris XI, Institut de Physique Nucléaire, 91406 Orsay Cedex, France, Commissariat à l'Energie Atomique/Valrhô, DEN/DRCP/SCPS, 30207 Bagnols sur Ceze Cedex, France, and Forschungszentrum Rossendorf, 01314 Dresden, Germany, at Rossendorf Beam Line/European Synchrotron Radiation Facility, 38043 Grenoble, France

Received July 25, 2005

The present work describes the first structural studies of protactinium(V) in sulfuric and hydrofluoric acid media using X-ray absorption spectroscopy. The results show unambiguously the absence of the *trans*-dioxo bond that characterizes the other early actinide elements such as U and Np. In concentrated sulfuric acid (13 M), Pa(V) is proved to exhibit a single oxo bond as postulated in the literature for species in more dilute media. In a 0.5 M HF medium, XANES and EXAFS spectra indicate the absence of any oxo bond: Pa(V) exists in the form of a pure fluoro complex.

Introduction

The physical−chemical properties of actinide elements strongly depend on the 5f/6d electronic configuration. Some of them (U, Np, Pu, and Am) can form AnO_2^{n+} ($n = 1$ and 2) oxocations, so-called actinyls, with two strong An−O bonds. Protactinium, as the first actinide with 5f electrons involved in bonding, occupies a key position in the actinide series. At formal oxidation state V (its most stable oxidation state in solution as well as in the solid state), Pa(V) corresponds to the formal $5f^5$ electronic configuration. U(VI) also corresponds to the formal oxidation state $5f^5$ and is most often encountered as the stable oxocationic form UO_2^{2+}. The first stable form of U, Np, or Pu at formal oxidation state V under atmospheric conditions is Np(V). It is encountered as NpO_2^+ with the formal $5f^5$ electronic configuration. On the contrary, the existence of the PaO_2^+ form in solution and in solid state is highly improbable, although it has been postulated by Welch[1] from cation-exchange experiments. In that way, the physical−chemical behavior of Pa(V) bears no resemblance to its heavier neighbors in the periodic classification Np and Pu at the same oxidation state. The main feature of Pa(V) aqueous chemistry is its strong tendency toward hydrolysis and colloid and polymer formation, especially in the absence of strong complexing ligands. This is reflected in a controversial literature based on scarce thermodynamic as well as structural data.[2,3] For instance, polymerization reactions are known to occur, with unpredictable induction time, except in HF and perhaps H_2SO_4 solutions.

Some analogies between Pa and group 5 elements (Nb and Ta) at the oxidation state V have been reported. Although the existing information on Nb and Ta species in aqueous solution is also scarce, the occurrence of a single terminal oxo group has been proposed at oxidation state V.[4] In the solid state, it is well-known that a short Nb−O oxo bond occurs in the niobium(V) oxohalide series.[5] At tracer scale ($\sim 10^{-12}$ M) and for freshly prepared solutions, Pa(V) in inorganic acid ($HClO_4$, HNO_3, HCl, or H_2SO_4) exists under a mixture of oxo/hydroxo forms in equilibrium.[6] In acidic noncomplexing media ($HClO_4$), the assumed species are $PaO(OH)^{2+}$, $PaO(OH)_2^+$, and $Pa(OH)_5$. In complexing media (HCl or H_2SO_4), the presence of a Pa−O bond has been postulated mainly from spectrophotometric measurements in

* To whom correspondence should be addressed. E-mail: christophe.denauwer@cea.fr.
[†] Institut de Physique Nucléaire.
[‡] Commissariat à l'Energie Atomique/Valrhô, DEN/DRCP/SCPS.
[§] Forschungszentrum Rossendorf, 01314 Dresden, Germany, at Rossendorf Beam Lin/ESRF.

(1) Welch, G. A. *Nature* **1953**, *172*, 458−458.
(2) Brown, D.; Maddock, A. G. *Quart. Rev.* **1963**, *XVII* (3), 289−341.
(3) Muxart, R.; Guillaumont, R. In *Compléments au nouveau traité de chimie minérale*; Masson, Ed.: Paris, France, 1974.
(4) Keller, O. L., Jr. *Inorg. Chem.* **1963**, *2*, 783−787.
(5) Giricheva, N. I.; Girichev, G. V. *J. Mol. Struct.* **1999**, *484*, 1−9.
(6) Guillaumont, R.; Bouissières, G.; Muxart, R. *Actinides Rev.* **1968**, *1*, 135−163.

10.1021/ic0512330 CCC: $30.25
Published on Web 11/08/2005

the UV region (~200−210 nm). However, in this region absorption of mineral acids may interfere.[2] In H_2SO_4 higher than 4−5 M, the postulated species are $Pa(SO_4)_3^-$ and $Pa(SO_4)_4^{3-}$, while in HCl media with concentration higher than 4 M, anionic complexes with or without an oxygen atom have been proposed: $PaOCl_5^{2-}$, $Pa(OH)Cl_6^{2-}$, $PaOCl_6^{3-}$, $PaCl_6^-$, and $PaCl_7^{2-}$.[3] More reliable results have been collected in HF media because fluoro complexes of Pa(V) have been proved to be stable toward hydrolysis: the complex PaF_7^{2-} is predominant in fluoride solutions, and its existence has been established with the synthesis and characterization of K_2PaF_7.[7]

The work presented in this paper is the first attempt to investigate the occurrence of the oxocation form of Pa(V) in HF and H_2SO_4 solutions. Sample **I** corresponds to Pa(V) in 0.5 M HF and sample **II** corresponds to Pa(V) in 13 M H_2SO_4. Comparison with two *trans*-dioxo cations of the actinyl family $U(VI)O_2^{2+}$ and $Np(V)O_2^+$ is discussed by means of X-ray absorption spectroscopy (XAS) data. Both regimes of the absorption coefficient have been used: XANES is a fingerprint of the absorbing atom's first-coordination sphere and is remarkably sensitive to well-known resonant scattering processes in *trans*-dioxo linear species; EXAFS corresponds to modulations of the absorption coefficient and contains structural information about the cation ligation mode.

Experimental Section

Sample Preparation. The separation of ^{231}Pa from its first three daughters (^{227}Ac, ^{227}Th, and ^{223}Ra) was performed using an anion-exchange AG-MP1 resin from Bio-Rad (100−200 mesh). All dishes as well as the self-made columns were Teflon-made, tubes in high-density polyethylene and tubings in Viton in order to limit material losses by adsorption. Samples of 10−20 mg of ^{231}Pa from IPN Orsay stock were dissolved in a small amount of ~10 M HCl, and the solution was slowly percolated onto the column. Under these conditions, Pa is quantitatively sorbed on the resin, whereas its decay products (Th, Ac, and Ra) pass through.[2,8] The elution of Pa was conducted with a mixture of 0.1 M HF/8 M HCl, leaving iron contamination on the column. Iron was then eluted with 1 M HCl and its presence confirmed by thiocyanate complexation. The eluted Pa fractions were evaporated to dryness, and the residue was taken up in a known volume of 11 M HCl. The ^{231}Pa concentration was determined by γ-ray spectrometry. Aliquots corresponding to the Pa amount required for XAS measurements (~1.7 mg) were evaporated in Teflon crucibles. For sulfuric and hydrofluoric samples, each residue was dissolved in 300 μL of 5 M $HClO_4$, evaporated until no more emission of white fumes was observed, and finally taken up in 700 μL of 0.5 M HF (sample **I**) or 13 M H_2SO_4 (sample **II**). Spectrophotometric data were recorded at room temperature with a Shimadzu 3101 spectrophotometer. Sample **I** shows no absorbance from the visible region to 210 nm, whereas sample **II** exhibits a strong absorbance from 320 to 220 nm. However, the region below 220 nm is complicated by interference with the absorption of mineral acids.[2]

Gamma spectra of samples **I** and **II** show the four main emission lines of ^{231}Pa at 283.67, 300.08, 302.07, and 330.07 keV and negligible contribution from ^{227}Th and ^{223}Ra impurities. The Pa concentrations deduced from these measurements are 6.82×10^{-3} M for sample **I** and 1.14×10^{-2} M for sample **II**.

XAS Data Acquisition and Treatment. XAS measurements were performed on samples **I** and **II** in 600-μL cells specifically designed for radioactive samples. XAS measurements of Pa were carried out on the Rossendorf Beam Line (ROBL)[9] at ESRF (6.0 GeV at 200 mA) in fluorescence mode, at room temperature, with a Si(111), water-cooled monochromator in a channel-cut mode. Two Pt-coated mirrors were used for harmonic rejection. Energy calibration was carried out with a Y foil (17 052 eV at the absorption maximum). All spectra were acquired at the Pa L_{III} edge (16 733 eV). XAS measurements of U and Np were carried out on the 11-2 Beam Line at SSRL (3.0 GeV at 100 mA) in fluorescence mode. See ref 10 for details. Data treatment (AUTOBK normalization) was done with Athena[11] code. Data fitting was carried out with Artemis[11] code in *R* space between 1.0 and 3.5 Å without any prior data filtering (Kaiser window between 2 and 12 $Å^{-1}$ for sample **I** and between 2 and 11 $Å^{-1}$ for sample **II**). Phases and amplitudes were calculated by Feff82[12] code from crystal structures of $RbPaF_6$[13] for sample **I** and $Na_{10}[(UO_2)(SO_4)_4](SO_4)_2 \cdot 3H_2O$[14] (with $Z = 92$ replaced by $Z = 91$ in the Feff input file) for sample **II**. Multiple scattering paths were included in the fit of **II**: triangular paths originating from the bidentate sulfates, collinear tripe, and quadruple paths originating from the monodentate sulfates. During the fit of **II**, the sulfate groups were considered as rigid tetrahedra. Therefore, only the Pa−O distances were allowed to vary, and the corresponding Pa−S distances and associated multiple scattering paths were linked to the corresponding Pa−O.

Results and Discussion

Figure 1 presents the L_{III} edge XANES spectra of samples **I** and **II** compared to $U(VI)O_2^{2+}$ in 0.1 M perchloric acid and $Np(V)O_2^+$ in 0.01 M perchloric acid.[10] XANES analysis of actinyl species has extensively been reported from both qualitative and quantitative approaches. Feature A corresponds to the so-called white line formally associated with the dipolar $2p^66d^0-2p^56d^1$ electronic transition. It is a signature of the empty states with 6d character of the cation. Feature B occurs in the spectra of the uranyl and neptunyl species. It is well-known to be due to resonant scattering along the linear *trans*-dioxo unit.[15] The absence of feature B in both experimental spectra of samples **I** and **II** precludes the occurrence of two trans Pa−O oxo bonds. Feature C is a shape resonance attributed to scattering from the equatorially coordinated ligands. Qualitatively, a shift of C to higher energy (C′) corresponds to a shortening of the equatorial bond length. To rationalize the above observations, XANES simulations (FDMNES code[16]) have been undertaken. The

(7) Brown, D.; Easey, J. F. *J. Chem. Soc. A* **1966**, 254−258.
(8) Suzuki, S.; Inoue, Y. *Bull. Chem. Soc. Jpn.* **1966**, *39* (3), 490−497.
(9) Matz, W.; Schell, N.; Bernhard, G.; Prokert, F.; Reich, T.; Claussner, J.; Oehme, W.; Schlenk, R.; Dienel, S.; Funke, H.; Eichhorn, F.; Betzl, M.; Pröhl, D.; Strauch, U.; Hüttig, G.; Krug, H.; Neumann, W.; Brendler, V.; Reichel, P.; Denecke, M. A.; Nitsche, H. *J. Synchrotron Radiat.* **1999**, *6*, 1076−1085.
(10) Den Auwer, C.; Guillaumont, D.; Guilbaud, P.; Conradson, S. D.; Rehr, J. J.; Ankudinov, A.; Simoni, E. *New J. Chem.* **2004**, *28*, 929−939.
(11) Ravel, B.; Newville, M. *J. Synchrotron Radist.* **2005**, *12*, 537−541.
(12) Rehr, J. J.; Albers, R. C. *Rev. Mod. Phys.* **2000**, *72*, 621−654.
(13) Burns, J. H.; Levy, H. A.; Keller, O. L., Jr. *Acta Crystallogr., Sect B: Struct. Crystallogr. Cryst. Chem.* **1968**, *B24*, 1675−1680.
(14) Burns, P. C.; Hayden, L. A. *Acta Crystallogr. Sect. C: Cryst. Struct. Commun.* **2002**, *C58*, i121−i123.
(15) Hudson, E. A.; Rehr, J. J.; Bucher, J. *J. Phys. Rev. B* **1995**, *52*, 13815−13826.
(16) Joly, Y. *Phys. Rev. B* **2001**, *63*, 125120−125130.

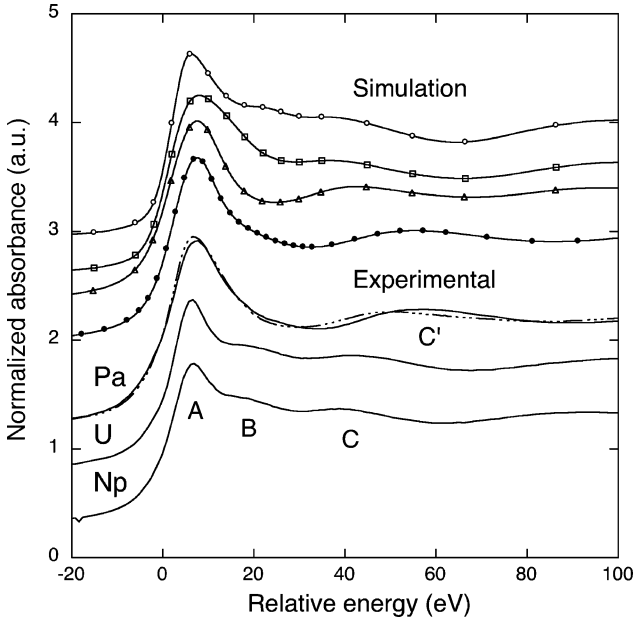

Figure 1. Experimental and simulated L_{III} edge XANES spectra of Pa(V), U(VI), and Np(V) species. For the sake of clarity, all spectra have been shifted with respect to the inflection point energy. (Top set) Simulated spectra of aqueous uranyl with successive removal of oxo oxygen atoms: (○) cluster of $UO_2(H_2O)_5$ (see ref 10 for details on the cluster used for simulation); (□) cluster of $UO(H_2O)_6$; (△) cluster of $U(H_2O)_7$. Note that no atom charge or cluster charge has been included in the simulation. The simulation of a cluster of PaF_7 using the Pa−F distances determined by EXAFS is also presented (●). (Bottom set) Experimental spectra of Pa(V), U(VI), and Np(V) species in aqueous solution: (—) sample **I** [Pa(V) in a HF solution]; (—···—) sample **II** [Pa(V) in a H_2SO_4 solution]; (—) UO_2^{2+} in a 0.1 M perchloric solution; (—) NpO_2^+ in a 0.01 M perchloric solution.

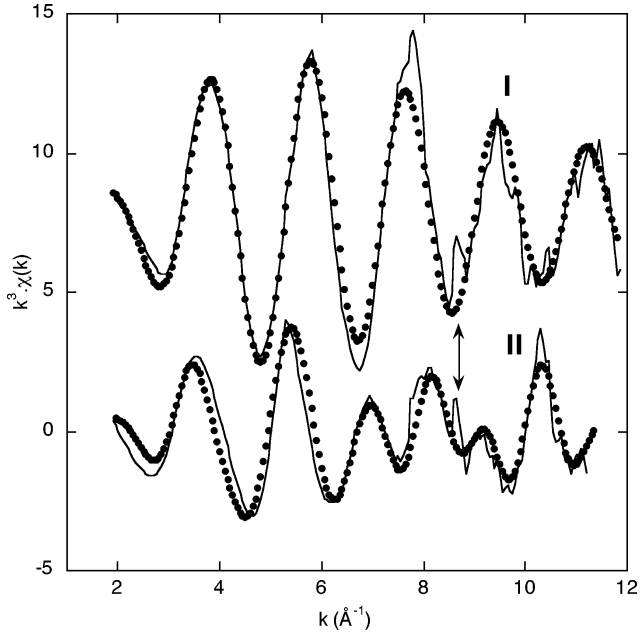

Figure 2. Experimental (—) and fitted (●) L_{III} edge EXAFS spectra of sample **I** (HF solution) and sample **II** (H_2SO_4 solution). The arrow indicates the presence of a glitch in the spectra.

calculation started from a well-known bipyramidal pentagonal cluster of $UO_2(H_2O)_5$ (with $U-O_{ax} = 1.77$ Å and $U-O_{eq} = 2.42$ Å).[10] Successive removal of one and two axial oxygens in the oxocation and replacement by H_2O at 2.42 Å were performed, leading to the two clusters $UO(H_2O)_6$, and $U(H_2O)_7$. A dramatic decrease of the feature B intensity in the first step and disappearance in the second step are observed upon breaking of the *trans*-dioxo geometry. Comparison between the simulations and experimental spectra of **I** and **II** confirms the absence of two linear Pa−O oxo bonds in the Pa(V) samples. However, given the core hole lifetime broadening at the Pa L_{III} edge (7.3 eV), it might be difficult to distinguish a coordination mode including one oxocation from a pure H_2O coordination. Moreover, the position of C′ in the experimental spectra of **I** and **II** compared to the position of C in the simulations indicates that the distance between Pa and the equatorial oxygen (O_{eq}) should be shorter than the $U-O_{eq}$ distance of 2.42 Å observed in $UO_2(H_2O)_5$. An additional XANES simulation has been carried out for sample **I**, using a cluster of one Pa atom surrounded by seven F atoms at a distance of 2.16 Å (cf. the EXAFS results in the next section). The agreement between simulated and experimental spectra of sample **I** is good: all of the features are well reproduced in position and amplitude.

Figure 2 presents the Pa L_{III} edge EXAFS spectra of **I** and **II**. Parts a and b of Figure 3 present the modulus and imaginary part of the corresponding Fourier transforms (FTs). Although attribution of the FT features in terms of atomic scatterers can be ambiguous because of the intricate constructive and destructive interferences, it will be used here for the sake of clarity. The FT of sample **I** exhibits a single peak, H, related to a monotonic sinusoidal EXAFS signal without any interference features. This peak indicates that only one type of backscatter contributes to the signal. According to the literature,[6,7,13,17,18] seven to nine fluoride ligands have been assumed to be in the first-coordination sphere. Best-fit parameters given in Table 1 have been obtained with seven fluoride ligands positioned at 2.16(2) Å. Note that, in the absence of a model compound, coordination numbers are difficult to estimate. A similar fit can be obtained with CN = 8, suggesting that the Pa coordination number falls in the 7−8 range. Note also that, because of their similar atomic numbers, F and O give very similar EXAFS signals, and therefore the results of the EXAFS experiment do not preclude the presence of water molecules in the Pa first-coordination sphere. Because fluoro complexes of Pa(V) have been proven to be stable toward hydrolysis, results about Pa(V) behavior in fluoride media described in the literature are more reliable. In HF concentrations ranging from 10^{-3} to 4 M, they report the complex PaF_7^{2-} to be predominant,[2,6] in agreement with the above findings. Furthermore, solid-state protactinium fluorides such as K_2PaF_7 have been reported as early as in the 1930s by Van Grosse.[19] Synthesis and characterization of this compound were later confirmed by Brown and co-workers.[7,17] The Pa−F distances obtained by EXAFS can hardly be compared to distances obtained for solid structures such as Na_3PaF_8 (2.21 Å),[18] $RbPaF_6$ (2.09 + 2.34 Å),[13] and K_2PaF_7

(17) Brown, D.; Smith, A. J. *Chem. Commun.* **1965**, *21*, 554−555.
(18) Brown, D.; Easey, J. F.; Rickard, C. E. *J. Chem. Soc. A* **1969**, 1161−1164.
(19) Von Grosse, A. *J. Am. Chem. Soc.* **1934**, *56*, 2501−2501.

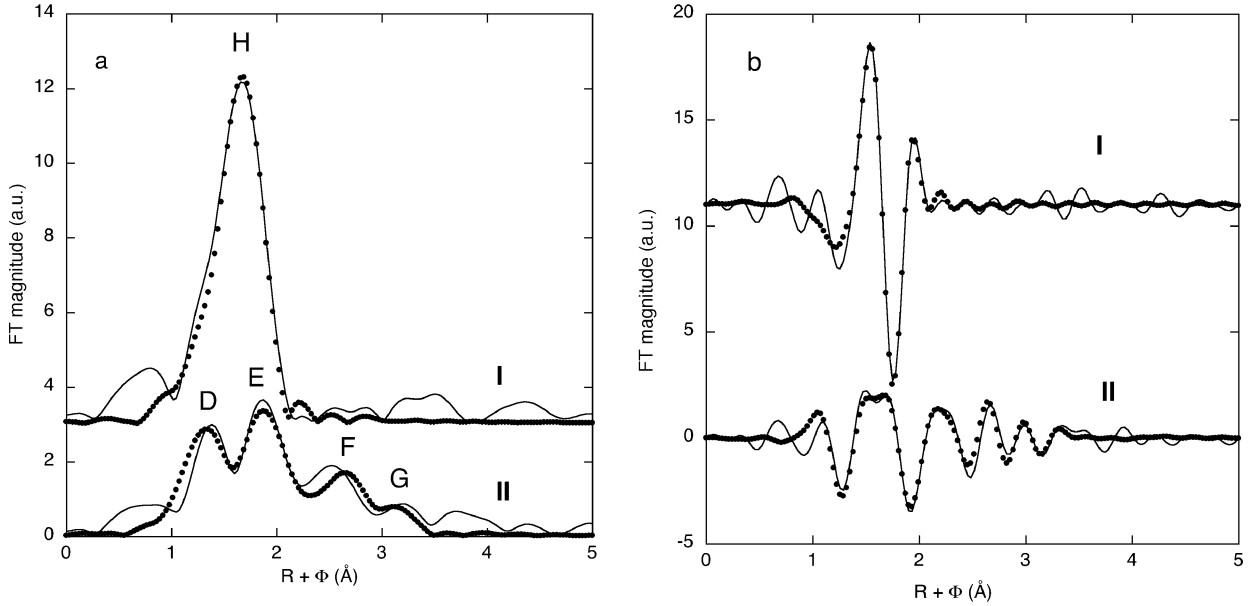

Figure 3. FTs of the L_{III} edge EXAFS spectra of samples **I** (HF solution) and **II** (H_2SO_4 solution). (a) Experimental modulus of the FT (not phase-shift-corrected) (thick —) and fitted curve (●). (b) Experimental imaginary parts of the FT and fitted curve (●).

Table 1. Best-Fit Parameters Obtained from the EXAFS Data Adjustment[a]

sample	coordination shell	
I (HF solution)	*7* F at 2.16(2) Å, $\sigma^2 = 0.0050$ Å^2	$S_0^2 = 0.83$
		$\Delta E_0 = 3.6$
		R factor = 2.6%
II (H_2SO_4 solution)	1 O at 1.72 Å, $\sigma^2 = 0.0030$ Å^2	$S_0^2 = 0.80$
	4 $O(SO_4)^{bid}$ at 2.41 Å, $\sigma^2 = 0.0102$ Å^2	$\Delta E_0 = 8.3$
	2 $S(SO_4)^{bid}$ at *3.09* Å, $\sigma^2 = 0.0023$ Å^2	R factor = 6.5%
	3 $O(SO_4)^{mon}$ at 2.33 Å, $\sigma^2 = 0.0120$ Å^2	
	3 $S(SO_4)^{mon}$ at *3.73* Å, $\sigma^2 = 0.0077$ Å^2	

[a] Multiple scattering paths included in the fit of **II** are not reported in the table. Numbers in italics were fixed or linked to variables during the fit.

(2.22 + 2.46 Å),[7] in which the Pa coordination sphere is highly distorted because of lattice constraints. On the other hand, simple bond distance estimation using Shannon's[20] ionic radii indicates that six-coordinate Pa(V) yields a Pa−F distance of 2.11 Å and eight-coordinate Pa(V) yields a Pa−F distance of 2.24 Å. The EXAFS result (2.16 Å) falls in this range.

For sample **II**, peak D in Figure 3a is attributed to a short Pa−ligand bond. This result agrees with the XANES experimental data and simulations of Figure 1 and is interpreted as strong evidence for the existence of a single short Pa−O bond in a monooxo form. Peak E reflects second-sphere O ligands, and peak F originates from third-sphere S ligands. In this scheme, peak G would correspond to multiple scattering contributions from the monodentate sulfate ligands. Adjustment of the EXAFS spectrum was carried out according to the general formula $PaO(SO_4)^{bid}{}_n$-$(SO_4)^{mon}{}_p$ (bid = bidentate; mon = monodentate) from n = 0−3 and p = 0−7. Because the coordination number in the equatorial plane of actinyls falls essentially between 5 and 6, between six and seven ligands are estimated to be coordinated to the Pa−O moiety ($2n + p = 6$ and 7). In the fits, sulfate ions were considered as rigid ligands according to the crystal structure of $Na_{10}[(UO_2)(SO_4)_4](SO_4)_2 \cdot 3H_2O$.[14] Multiple scattering paths were included in the fit and linked to the first-neighbor distances, as described in the Experimental Section. Fits with only bidentate or only monodentate sulfate ligands did not reproduce the experimental spectrum. Fits with $n = 1$, $p = 4$ or $n = 3$, $p = 1$ led to poor agreement. The optimum number for n was found to be 2 (four oxygen atoms coming from two bidentate sulfate ligands). Within the uncertainty associated with the amplitude estimation in EXAFS, the fit is more sensitive to number n than to number p because n contributes for two oxygen atoms and one sulfur atom. Backscattering from the sulfur atom also contributed to the determination of n. The value of p was then fixed to 3 according to the assumption that $2n + p = 6$ and 7. However, the uncertainty was about ±1. Best-fit structural parameters presented in Table 1 were obtained with one Pa−O bond at 1.72(2) Å, two bidentate sulfate ligands at 2.41(2) Å with corresponding S atoms at 3.09 Å, and three monodentate sulfate ligands at 2.31(2) Å with corresponding S atoms at 3.72 Å. The high Debye−Waller values of the $O(SO_4)$ contributions may indicate that water molecules can also contribute to the Pa coordination sphere. The R factor is only equal to 6.5% because peak F is poorly reproduced in the modulus of the FT. The poor agreement obtained on peak F is attributed to an amplitude discrepancy between the fit and the experiment because the imaginary parts of the FT in Figure 3b are in very good agreement. The presence of a glitch in the EXAFS curves (arrow in Figure 2) may also contribute to an increase of the R factor. In conclusion,

(20) Shannon, R. D. *Acta Crystallogr., Sect. A: Cryst. Phys., Diffr., Theor. Gen. Crystallogr.* **1976**, *32*, 751−767.

the results indicate unambiguously the presence of one oxo bond in a 13 M H_2SO_4 medium, as postulated for more dilute media where the species $PaOSO_4^+$ and $PaO(SO_4)_2^-$ have been proposed.[3,6] Furthermore, the number of mono- and bidentate sulfate ligands deduced from EXAFS agrees with one of the formulations of oxotrisulfatoprotactinate(V) proposed by Bagnall et al. [21]

Conclusion

XAS experiments on Pa(V) in HF and concentrated H_2SO_4 solutions have demonstrated the absence of any *trans*-dioxo bond in Pa(V) species, in contrast with other heavier actinides such as U, Np, or Pu. For the first time, the existence of a single Pa−O oxo bond in aqueous solution has been demonstrated unambiguously. The presence of this bond in concentrated H_2SO_4 contrasts with the Pa species proposed in the literature because the mixed oxosulfato complexes are assumed to exist only until 4 M H_2SO_4.[3] On the other hand, the absence of the oxo bond in the HF medium agrees well with the literature data, in solution and at the solid state. Further XAS experiments at other concentrations and in other acidic media as well as theoretical calculations are in progress in order to complete our knowledge on the coordination chemistry of actinides.

Acknowledgment. Support for this research was provided by the ACTINET program (Grant JRP-02-19), a European network for actinide sciences, and Groupement de Recherche PARIS, France. XAS measurements were carried out at ESRF, a European user facility, and at Stanford Synchrotron Radiation Laboratory, a national user facility operated by Stanford University on behalf of the U.S. Department of Energy, Office of Basic Energy Sciences. The authors thank A. Scheinost, H. Funke, and A. Rossberg (ESRF/ROBL), J. Bargar and J. Rogers (SSRL/11-2), and S. D. Conradson (LANL) for their help.

IC0512330

(21) Bagnall, K. W.; Brown, D.; Jones, P. J. *J. Chem. Soc.* **1965**, *27*, 176−181.